Appendix E
Pushover Analysis of Pile-Founded Navigation Locks

E-1. Introduction

a. This appendix provides an example pushover analysis for a pile-founded navigation lock. The example lock is Olmsted Locks and Dam located on the Ohio River near town of Olmsted, Illinois. The lock structure consists of two 33.5-m by 365.8-m (110-ft by 1200-ft) locks supported by more than 11,700 H-piles (HP 14x117). The H-piles are 12.2 to 13.7 m (40 to 50 ft) long and are spaced 1.5 to 2.1 m (5 to 7 ft) in the upstream-downstream direction and 1.8 to 3.8 m (6 to 12.5 ft) in the cross-stream direction. The Olmsted Locks were designed for the MDE ground motion with a return period of 1,000 years. The design calculations consisted of the seismic coefficient method as well as the dynamic soil-pile-structure-interaction (SPSI) procedure. In the SPSI analysis, the nonlinear soil behavior was approximated by the equivalent linear techniques described in EM 1110-2-6051, but the H piles and reinforced concrete were assumed to behave linearly.

b. In this example, the mathematical model of the lock incorporates inelastic material response, thus allowing for redistribution of forces and deformations as structural members undergo nonlinear response in the form of yielding and cracking. With increasing the magnitude of loading during the pushover analysis, weak links and failure modes of the lock structure are found. The results of static pushover analysis are summarized as a plot of lateral load vs. displacement (pushover or capacity curve), from which the actual load capacity and ultimate displacement of the structure can be determined.

E-2. Purpose and Objectives

The purpose of this example is to illustrate application of nonlinear static pushover analysis described in Paragraph 6.5b to performance evaluation of navigation locks founded on piles. The objectives of the pushover analysis are:

a. To compute concrete section and pile capacities

b. To obtain pushover curve showing yielding, cracking, and ultimate displacement of the lock

c. To identify the sequence of plastic hinging and potential failure modes

E-3. Scope

The scope of this example includes pushover analyses for two structural idealizations and involves the following:

a. Idealization of lock monoliths using frame elements

b. Idealization of soil-pile-foundation using lumped nonlinear springs (Lumped Model)

c. Idealization of soil-pile-foundation using nonlinear frame elements to represent the piles and nonlinear springs to model the soil (Full Model)

d. Conducting pushover analyses to obtain performance curves for the lumped and full models

e. Evaluation of results to assess inelastic response behavior and ultimate displacement capacities of the lock

E-4. Assumptions

The following assumptions were made to reduce the amount of calculations and better demonstrate the effects of most important parameters on the inelastic response.

a. Piles were modeled using lumped plasticity, where plastic hinges are assumed to form at the two ends of the element.

b. The effect of axial load on bending moment was ignored in developing section moment-curvature relationships for the piles.

c. Reinforced concrete members were modeled using fiber elements with distributed plasticity. The fiber elements are characterized by the constitutive models of the concrete and reinforcing steel.

d. In 3D structures, the axial load interacts with both the in-plane and out-of-plane bending moments (i.e. P-M_x-M_y). In 2D-pushover analysis, the structure is restricted to in-plane bending, and thus only axial load interaction with the in-plane bending moment was accounted for.

e. The P-δ effect is not considered.

f. The structure is assumed not to fail in shear.

E-5. Finite Element Models

a. The example lock is a typical chamber monolith section of the Olmsted Locks and Dam. It consists of lightly reinforced concrete slab floor and walls founded on steel piles producing two chambers, each 110 ft and 1 in. wide. The upper graph in Figure E-1 shows the basic geometry and dimensions of the chamber monolith.

b. For reasons of simplicity and available analytical capabilities, the nonlinear static pushover analysis is carried out using beam-column (frame model) idealization of the lock structure. To insure accuracy of this approach, the frame model was calibrated against a 2D finite-element (solid elements) representation of the lock. Two computer models, one based on 2D solid elements (Figure E-1, upper graph) and another using equivalent 2D beam-column elements (Figure E-1, lower graph) were developed and analyzed. The rigid panel zones in the frame model were adjusted to obtain the same or nearly the same deformations, vibration frequencies, and mode shapes for the two models. The lengths of rigid zones were selected based on the geometry, but their rigidity was determined by trial and error.

c. The final calibrated frame model is shown in Figure E-1 (lower graph). In this figure thick lines show the assumed rigid zones and fine lines represent the flexible beam-column elements. A rigidity factor of 1.0 was obtained from the equivalence analysis. Tables E-1 and E-2 show material properties and reinforcements for various lock sections, respectively.

d. The pushover analysis of the example soil-pile-lock system was performed using a two-dimensional slice. The depth or thickness of the slice was chosen such that the relative rigidities of the soil-pile-lock system are preserved. The pile spacing along the length of the lock is 2.13 m (7 ft). The thickness of the slice is chosen equal to the pile spacing so that pile forces and moments are obtained directly without scaling.

E-6. Section Strength Capacities and Moment-Curvature Relationship

Using the material properties listed in Table E-1, reinforcing steel listed in Table E-2, and dimensions indicated in Figure E-1, the lock section capacities were calculated. The results are presented in Table E-3 and Figure E-2. Based on geometry and amount of reinforcements, lock sections are grouped into six sections designated as Base-1, Base-2, Beam-2, Col-1, Col-2, and Col-3, as shown in Figure E-1. The reinforcing steel ratios for these sections vary from the lowest 0.3 percent for Col-3 to the highest 0.8 percent for Col-1. Computer program "*M-phi*" (Ehsani and Marine 1994) was used to estimate strength capacities and moment-curvature relationship for each of the sections. The *M-phi* moment-curvature relationships were estimated for verification of the same obtained by fiber elements, as discussed later in Paragraph E-10b. The results show that the cracking moments for all concrete sections are 2 to 3 times smaller than the nominal moments, except for Col-3 section whose cracking moment is only slightly lower than the corresponding nominal moment. Figure E-2 shows moment-curvature relationships computed for various lock sections. This provides information necessary for evaluation of the inelastic response of the lock when the lumped plasticity model is used. The concrete cracking and steel yielding for each section can easily be identified on this figure.

Table E-1. Assumed material properties

Parameter		Value	
Re-bar Material Properties			
Modulus of Elasticity	(E_s)	199,958.46 MPa	29,000.00 ksi
Specified Yield Strength	(f_y)	413.71 MPa	60.00 ksi
Strain Hardening			0.80 %
Steel Ultimate Stress		517.13 MPa	75.00 ksi
Steel Ultimate Strain			5.00 %
Concrete Material Properties			
Modulus of Elasticity	(E_c)	23,457.77 MPa	3,402.08 ksi
Shear Modulus	(G)	9,774.07 MPa	1,417.53 ksi
Poisson's Ratio	(ν)		0.20
Concrete Compressive Strength	(f'_c)	20.69 MPa	3.00 ksi
Modulus of Rupture (per ACI)	(f_r)	2.83 MPa	0.41 ksi
Concrete Ultimate Strain	(ε_c)		0.30 %

Table E-2. Reinforcing steel properties

Section ID	Reinforcing Bar (per foot of depth)					
	Upper			Lower		
Base-1	1- #18	2.58 mm^2	4.00 in^2	1- #18	2.58 mm^2	4.00 in^2
Base-2	1- #18 & 1- #14	4.03 mm^2	6.25 in^2	1- #18 & 1- #14	4.03 mm^2	6.25 in^2
Beam-2	2- #11	1.82 mm^2	2.82 in^2	2- #11	1.82 mm^2	2.82 in^2
Col-1	2- #11	1.82 mm^2	2.82 in^2	2- #11	1.82 mm^2	2.82 in^2
Col-2	2- #11	1.82 mm^2	2.82 in^2	2- #11	1.82 mm^2	2.82 in^2
Col-3	2- #11	1.82 mm^2	2.82 in^2	2- #11	1.82 mm^2	2.82 in^2

Table E-3a. Calculated section capacities (English units)

Parameter		Base-1	Base-2	Beam-2	Col-1	Col-2	Col-3
Depth	b (ft)	7.00	7.00	7.00	7.00	7.00	7.00
Width	h (ft)	12.00	12.00	6.00	5.00	8.00	14.00
Section Area	A (ft^2)	84	84	42	35	56	98
Moment of Inertia	I_{yy} (ft^4)	1,008	1,008	126	73	299	1,601
Nominal Moment	M_n (k-ft)	18,771	28,847	6,241	5,057	8,610	15,717
Cracking Moment	M_{cr} (k-ft)	9,938	9,938	2,484	1,725	4,417	13,527
Shear Capacity	V_x (kips)	530,020	530,020	265,010	220,842	353,347	618,357
Tension Capacity	P_t (kips)	3,360	5,250	2,369	2,369	2,369	2,369
Compression Capacity	P_c (kips)	36,288	36,288	18,144	15,120	24,192	42,336

Table E-3b. Calculated section capacities (metric units)

Parameter		Base-1	Base-2	Beam-2	Col-1	Col-2	Col-3
Depth	b (m)	2.13	2.13	2.13	2.13	2.13	2.13
Width	h (m)	3.66	3.66	1.83	1.52	2.44	4.27
Section Area	A (m^2)	7.80	7.80	3.90	3.25	5.20	9.10
Moment of Inertia	I_{yy} (m^4)	8.70	8.70	1.09	0.63	2.58	13.82
Nominal Moment	M_n (kN-m)	25,451	39,113	8,463	6,857	11,674	21,310
Cracking Moment	M_{cr} (kN-m)	13,475	13,475	3,369	2,339	5,989	18,341
Shear Capacity	V_x (kN)	2,357,771	2,357,771	1,178,885	982,405	1,571,847	2,750,733
Tension Capacity	P_t (kN)	14,947	23,354	10,538	10,538	10,538	10,538
Compression Capacity	P_c (kN)	161,426	161,426	80,713	67,261	107,617	188,330

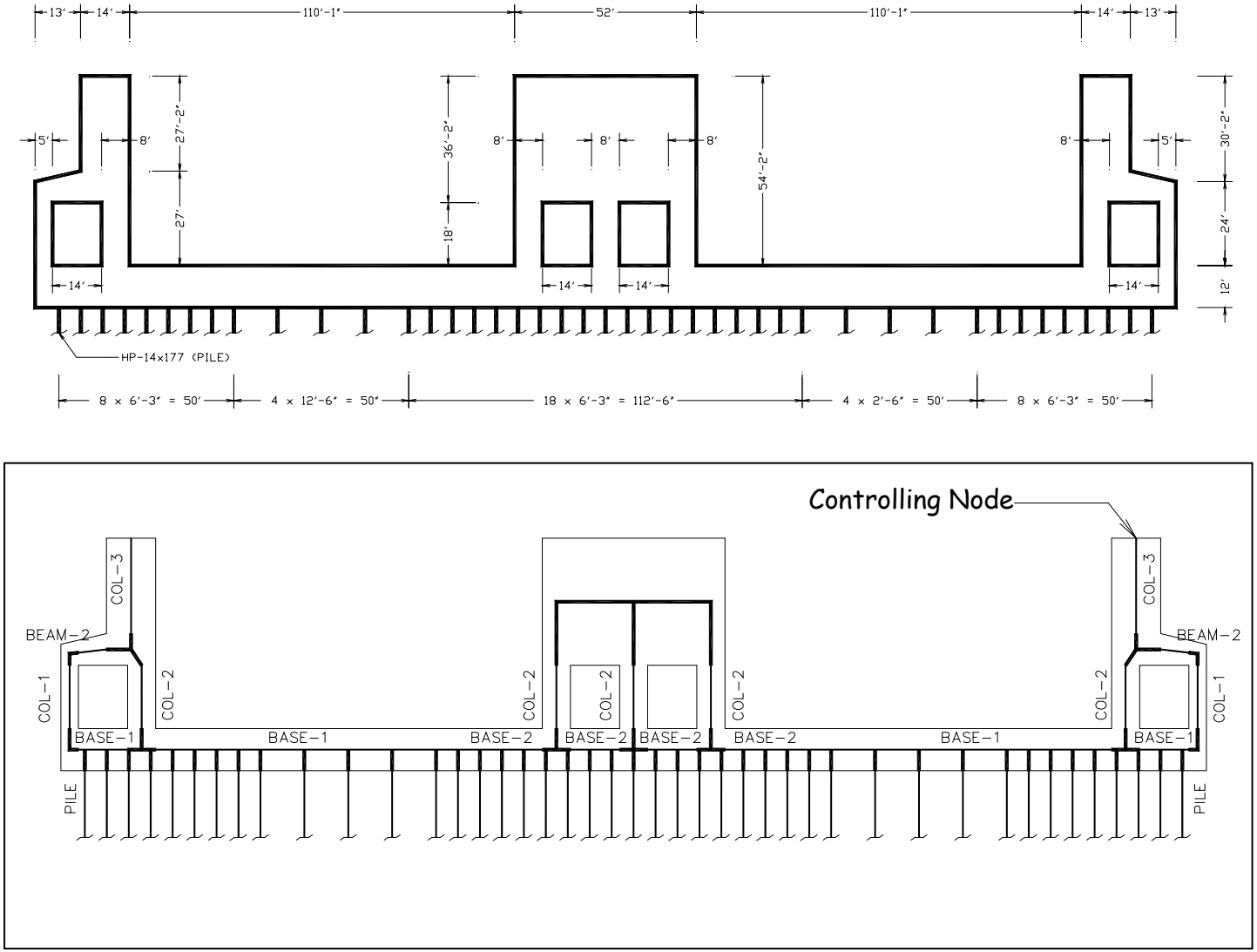

Figure E-1. Basic geometry and frame model of reinforced concrete lock

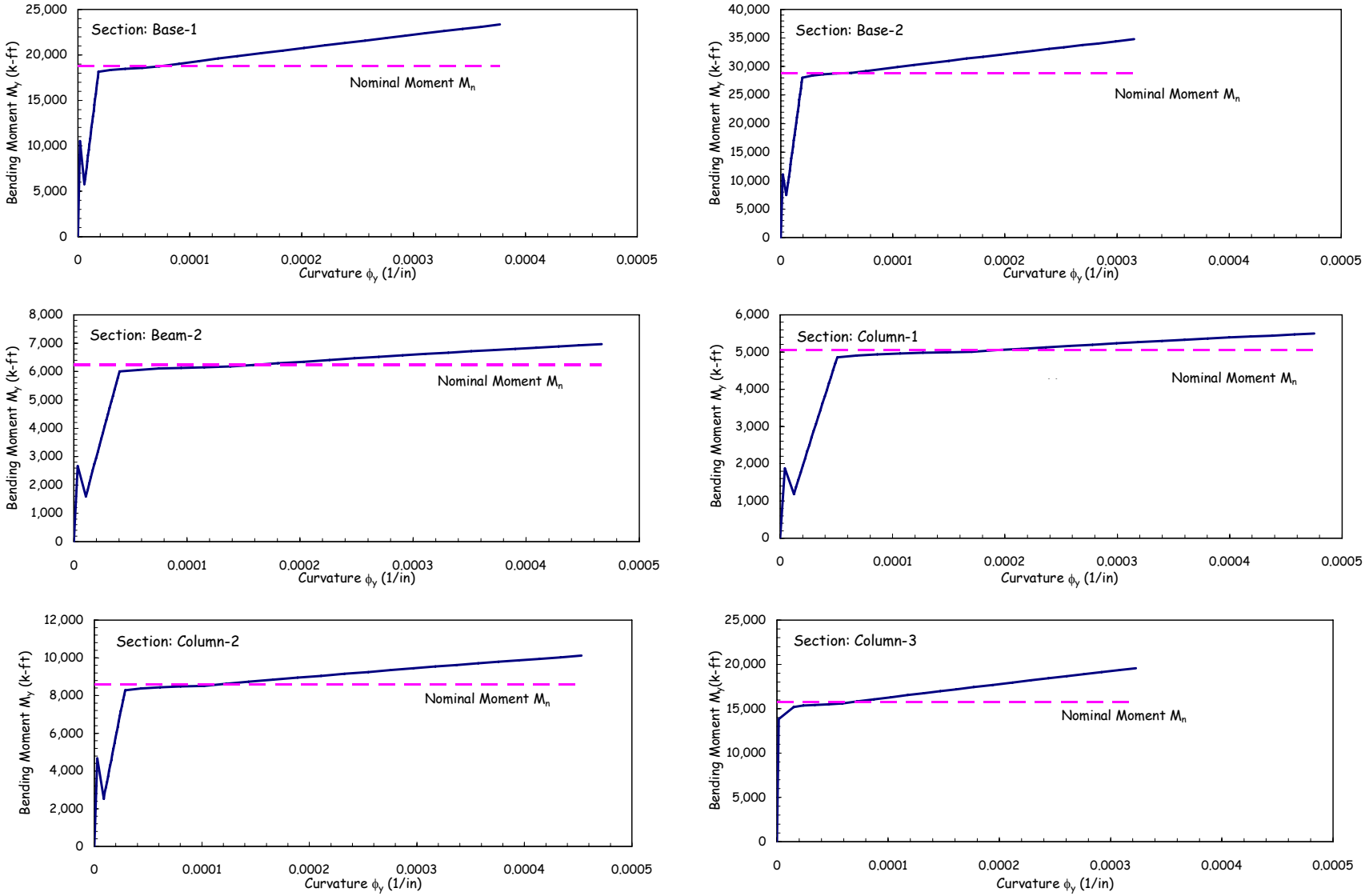

Figure E-2. Calculated moment capacities of various lock sections (shown in Figure E-1)

E-7. Analysis Procedures

a. Non-linear static pushover analysis implies monotonic application of static load to mathematical model of the structure. The load is applied in increments until the maximum load (load controlled) or a target displacement is reached (displacement controlled). This procedure requires considerably more analysis effort than does the linear static procedure. It is therefore conducted using a computer program having nonlinear analysis capabilities.

b. The maximum seismic load demands in the load-controlled pushover analysis cannot easily be determined. Consequently, the displacement-controlled method of analysis is commonly used to conduct pushover analysis. Accordingly, static lateral loads are applied incrementally to a mathematical model of the structure until a target displacement is exceeded. The target displacement represents the maximum displacement that the structure is likely to experience when subjected to the design earthquake. An estimate of target displacement for building structures is given by FEMA-356 (2000). The target displacement for lock structures has not been developed. Consequently, the step-by-step nonlinear pushover analysis for lock structures should continue until the resulting displacement is large enough to mobilize principal nonlinear mechanisms or the structure collapses.

c. The main objective of pushover analysis is to obtain a pushover or capacity curve by which performance of the structure can be assessed. The performance is considered satisfactory if permissible deformation and strength demands for a prescribed performance level are met. For deformation-controlled actions (such as flexural moment) deformation demands are compared with the maximum permissible values for the component. While for force-controlled actions (such as shear forces in beams) the force demands are compared with the strength capacity. If either the force demand in force-controlled elements or deformation demand in deformation-controlled members exceeds permissible values, then the element is deemed to violate the performance criteria. The applied load pattern should closely resemble the probable earthquake load pattern. As an example for structures whose response is governed by the fundamental mode of vibration, the lateral load pattern may be selected proportional to the fundamental mode shape of the structure. Since dynamic response of the example lock structure is dominated by the fundamental mode, it seems reasonable to assume a load pattern (i.e. lateral inertia forces) proportional to the product of fundamental mode shape and nodal masses. In other cases, a dominant load pattern may not exist. In those situations, two or more load patterns should be considered. It is also a good idea to normalize the load pattern such that the sum of all horizontal components is equal to unity. The benefit of such normalization is that the load scale factor, computed by some programs such as DRAIN-2DX (1994), directly gives the base shear.

d. To speed up the computations the size of computer model is reduced by replacing the pile-soil-foundation system with equivalent lumped pile-head stiffness. The pile-head stiffness is represented by sets of non-linear springs arranged at appropriate locations. This model referred to as the "Lumped Model" is discussed in Paragraph E-7*e*. The computation of pile-head stiffness coefficients is described in Section E-8. Alternatively, one may develop a complete pile-soil-foundation model using nonlinear frame elements to represent the piles and nonlinear springs to idealize the pile-soil foundation. This model referred to as the "Full Model" is discussed in Paragraph E-7*f*. Obviously, the Full Model requires significantly more computational efforts than does the Lumped Model, thus limiting the engineer's ability to perform parameter sensitivity study. The need for the parameter sensitivity study could frequently arise from the poor or lack of convergence of numerical algorithms. In this example, the Lumped Model was first used to perform initial analyses and to make any necessary

adjustments to the model before a Full Model could be developed and analyzed. In Paragraph E-10, the results from the Lumped and Full Models are discussed and compared to validate the assumptions regarding the Lumped Model.

e. Lumped Model. Figure E-3 shows a plot of lock model with the lumped pile-head system. *Load pattern* for this model is chosen as a product of the first mode shape and the corresponding nodal masses. The lateral loads that would have been acting along the length of piles are lumped at the location of each pile-head spring. The lateral load is applied to "push" the lock model to the left. The *controlling node*, at which the lateral displacement is monitored, is taken at the top of the right wall. A *target displacement* of 1.0 ft is selected.

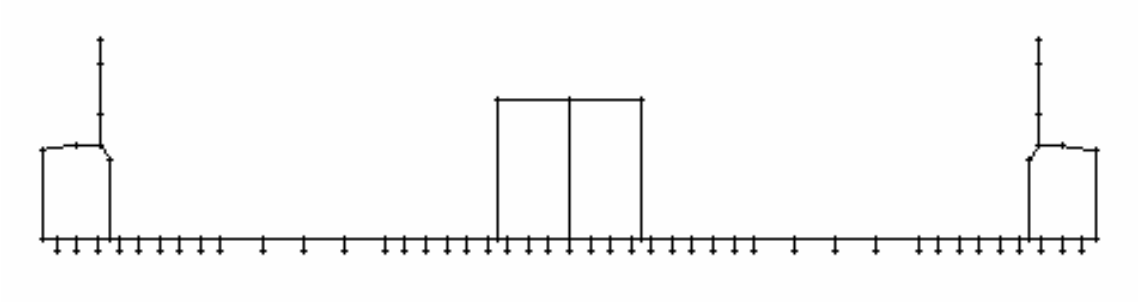

Figure E-3. Lumped pile-head model of reinforced concrete lock

f. Full Model. Figure E-4 shows a plot of lock model with the full pile-soil-foundation system. Each pile is represented by 11 nonlinear beam-column or frame elements supported by 11 lateral nonlinear soil springs. The nonlinear force-displacement relationship for soil springs are represented by *p-y* curves estimated for each soil layer. *Load pattern* for this model is also chosen as the product of the first mode shape and the corresponding nodal masses. The load pattern is applied to push the lock to the left. The *controlling node* is selected at the top of the right wall. A *target displacement* of 1.0 ft is selected.

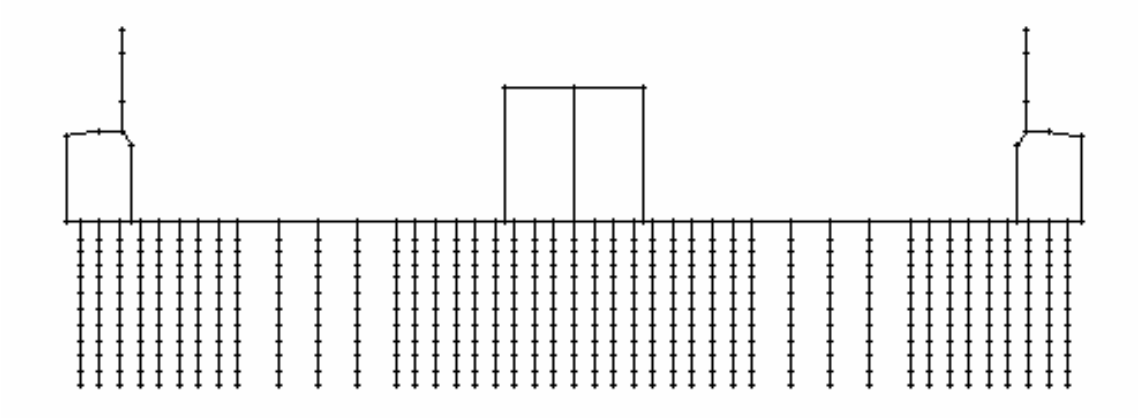

Figure E-4. Full model of reinforced concrete lock

E-8. Single Pile Analysis

a. This section describes computation of the equivalent pile-head stiffness used in the Lumped Model. The effects of pile-soil-foundation system can be approximated by sets of equivalent nonlinear springs attached to the base of the lock model. The stiffness of these springs is calculated by conducting a nonlinear static analysis of a single pile-soil model subjected to either a lateral load or moment. The pile is modeled with nonlinear beam-column elements and the soil is represented by nonlinear *p-y* curves. In the first analysis the pile head is constrained against the rotation and subjected to an incrementally increasing lateral load. A plot of lateral load versus lateral displacement produces the lateral stiffness K_{xx} shown in the upper left graph of Figure E-5. Whereas a plot of the induced pile-head moment as a function of the lateral displacement gives the coupling stiffness, $K_{\theta x}$ shown in the lower left graph of Figure E-5. In the second analysis the pile head is constrained against lateral displacement and subjected to incrementally increasing moment. A plot of the applied moment versus the rotation produces the nonlinear rotation stiffness, $K_{\theta\theta}$, shown in the lower right graph of Figure E-5. The applied moment generates a lateral reaction at the fixed pile head, which if plotted against rotation produces the coupling stiffness $K_{x\theta}$, as shown in the upper right graph of Figure E-5.

b. The presence of large off-diagonal terms in Figure E-5 suggests a strong coupling between the rotation and lateral stiffness. The incorporation of coupling stiffness terms in the analysis is not straightforward if the computer program lacks such capabilities. However, the coupling terms can be accounted for indirectly if the springs are placed at an offset equal to the ratio of $K_{\theta x}/K_{xx}$, as illustrated in Figure E-6. This ratio or offset remains constant within the linear-elastic range of behavior, but varies significantly in the inelastic deformation range.

c. Figure E-7 displays variation of offset *h* with respect to load steps. Since the location of springs (i.e. value of *h*) cannot be changed within a single computer run, some average value of *h* should be assumed. Separate analyses could also be run using either the maximum or the minimum *h* to envelop the results. Other approaches are to select *h* based on the expected deformations, or run several analyses with different possible values of *h*. All of these approaches, however, require several computer runs.

d. In this example, a single value of $h = 3.5$ was selected to avoid numerous computer runs, with the understanding that these results will later be compared with the Full Model for further validation.

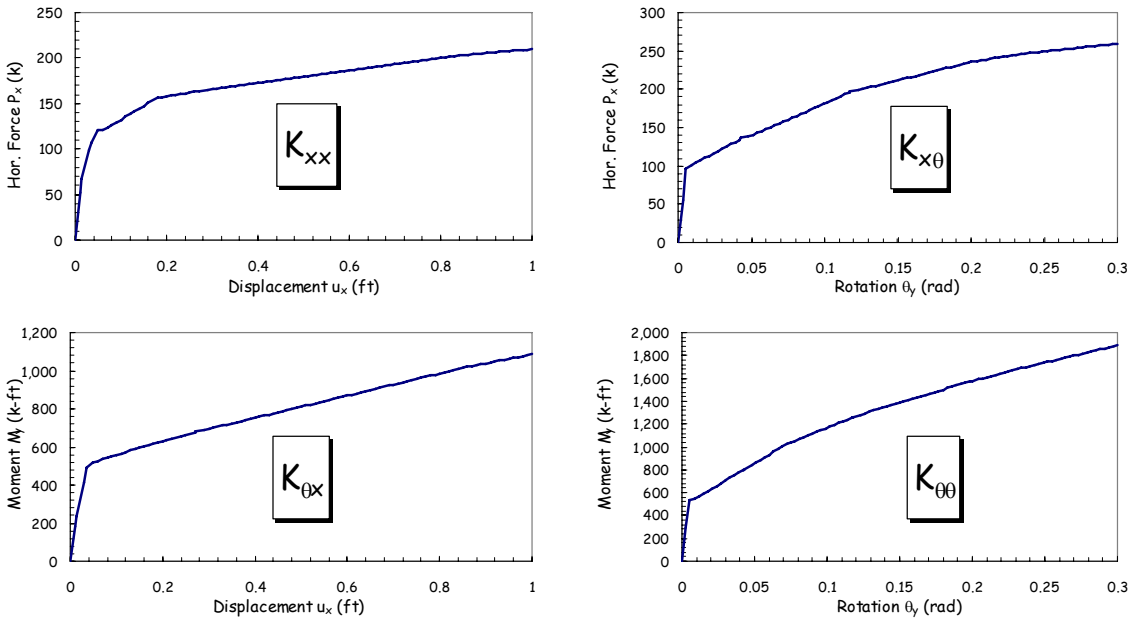

Figure E-5. Nonlinear pile-head stiffness matrix

$$\begin{Bmatrix} V_x \\ M_y \end{Bmatrix} = \begin{bmatrix} K_{xx} & K_{x\theta} \\ K_{\theta x} & K_{\theta\theta} \end{bmatrix} X \begin{Bmatrix} u_x \\ \theta_y \end{Bmatrix}$$

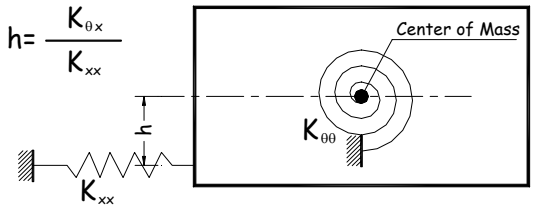

Figure E-6. Pile-head springs

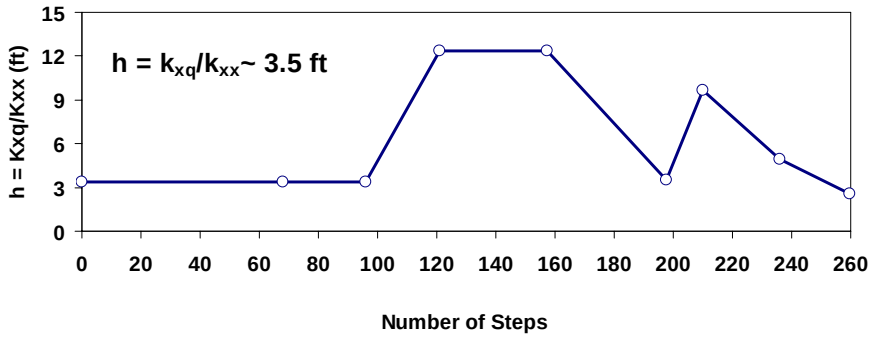

Figure E-7. Variation of offset *h* as a function of load step

E-9. Pushover analysis using computer program DRAIN-2DX

a. An enhanced version of the computer program DRAIN-2DX is used to illustrate the application of nonlinear static procedures to pushover analysis of navigation locks. Three types of elements are used to model the lock-pile-foundation system: 1) a distributed plasticity fiber beam-column element (Type 15), 2) a lumped plastic-hinge beam-column element (Type 02), and 3) a simple connection or spring element (Type 04). Fiber beam-column elements are used to model the reinforced concrete lock, as shown in Figures E-1, E-3, and E-4. Plastic-hinge beam-column elements are used to model steel piles. While simple connections or spring elements are used to represent the nonlinear soil.

b. Fiber Model. The reinforced concrete lock is represented using fiber beam-column elements available in DRAIN-2DX. Each lock section is divided into 18 concrete and 2 steel fibers, as shown in Figure E-8. This "distributed plasticity" modeling permits for the spread of inelastic behavior both over the cross section and along the member length (Campbell 1994). The fiber modeling is in contrast to a conventional "lumped plasticity" model, where the inelastic behavior is concentrated in zero length plastic "hinges." The use of fibers to model cross sections accounts rationally for axial force-moment interaction, while no yield surface or plastic flow rule needs to be defined explicitly. The concrete and reinforcing bars are represented by separate fibers, each with its own material properties, as shown in Figure E-9. Such model can account for yielding of steel including strain hardening, cracking and crushing of concrete including post-crushing strength loss, crack opening, and reinforcing bar pullout if desired. The same fiber model of the lock was used for the Lumped and Full Models of the pile-soil-foundation system.

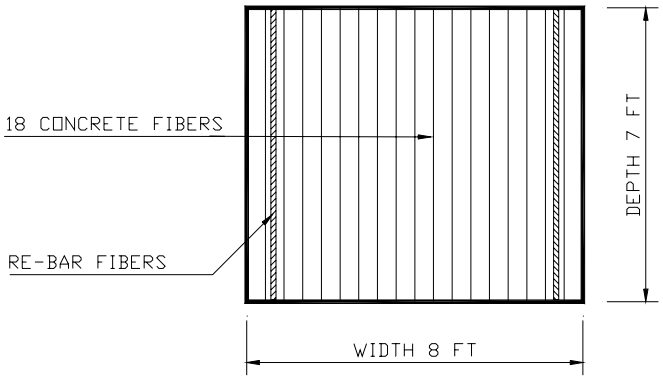

Figure E-8. Fiber element cross-section for Col-3

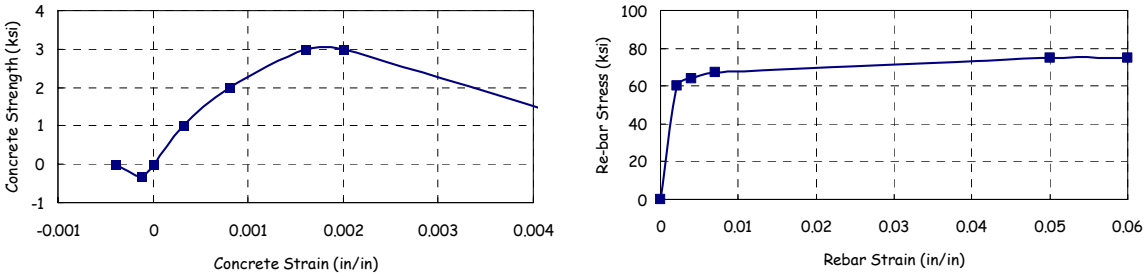

Figure E-9. Assumed stress-strain relationship for concrete and reinforcing bar

c. Lumped Plastic-Hinge Model. The conventional lumped plastic-hinge beam-column elements (Type 02 in DRAIN-2DX) were used to model steel piles in the Full Model representation of the pile-soil-foundation system. In the Full Model, the same nonlinear spring elements (Type 04 in DRAIN-2DX) discussed next were used to model the nonlinear soil along the length of piles. Except that the stiffness of the soil springs was based on the *p-y* curves.

d. Nonlinear Springs. The pile-soil-foundation system in the Lumped Model was modeled using nonlinear spring elements (Type 04 in DRAIN-2DX). The effects of each pile and the surrounding soil were represented by three sets of nonlinear springs estimated according to the procedure discussed in Section E-8. Each set of springs included a vertical, horizontal, and rotational springs. The horizontal and rotational springs were positioned with an offset according to Figure E-4 to produce coupling stiffness terms between lateral and rotational degrees of freedom.

E-10. Evaluation of Results

a. Deflected Shapes. Figures E-10 and E-11 show deflected shapes of the Lumped and Full Models respectively after being pushed to a target displacement of about 1 foot. Red symbols indicate the locations where nonlinear deformation takes place. Nonlinear behavior includes cracking and crushing of the concrete, yielding of the reinforcing steel, and yielding of the pile-soil foundation. A quick examination of Figure E-10 shows that all pile-head springs in the Lumped Model have yielded and that reinforced concrete sections have experienced cracking and yielding at the base slab and at the top of the lock walls. A yielding of the pile-head springs indicates a yielding of the steel piles, or soil, or both. Similarly the Full Model also indicates yielding of the piles with some cracking and yielding of the base slab but no cracking of the lock walls.

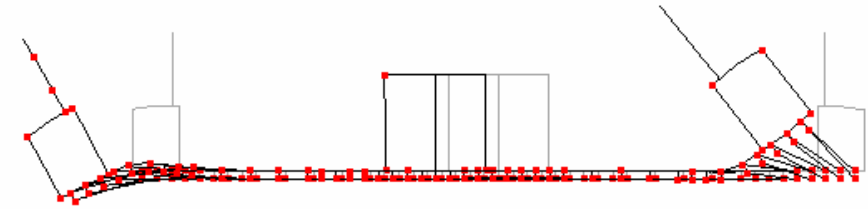

Figure E-10. Lumped model deflected shape

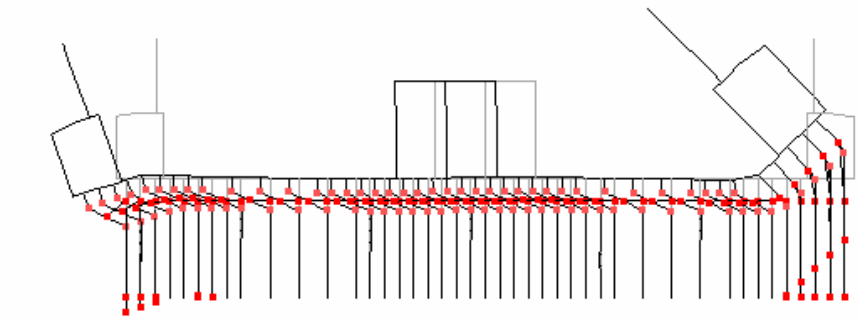

Figure E-11. Full model deflected shape

b. Moment-Curvature. A more detailed evaluation of the structural performance is carried out by a careful examination of the location, extent, and sequence of inelastic deformations. All sections and members exhibiting inelastic response are identified and their moment-curvature or force-displacement relationships are plotted and evaluated to assess the damage. The level of damage is then compared against the acceptance criteria. Figure E-12 is one such moment-curvature relationship for the base slab section of the lock. The figure compares moment-curvature relationships obtained from the Full Model, Lumped Model, and the *M-phi* program. The figure also includes the nominal bending moment as a reference. The results indicate that the concrete cracking starts at a bending moment of about 1,3558 kN-m (10,000 k-ft), followed by a stiffness reduction of the lock section due to cracking and yielding of reinforcing steel at about 27,116 kN-m (20,000 k-ft). The agreement among different models is quite reasonable. The difference between the *M-phi* and DRAIN-2DX fiber model is due to effects of shear and axial force inherent in the fiber model but not accounted for in the *M-phi* calculation of the section moment-curvature. The moment-curvature relationship in Figure E-12 is a measure of the local damage. The acceptance of local damage can be determined by comparing the induced inelastic curvature (or rotation) with the ultimate curvature or rotation capacity of the section.

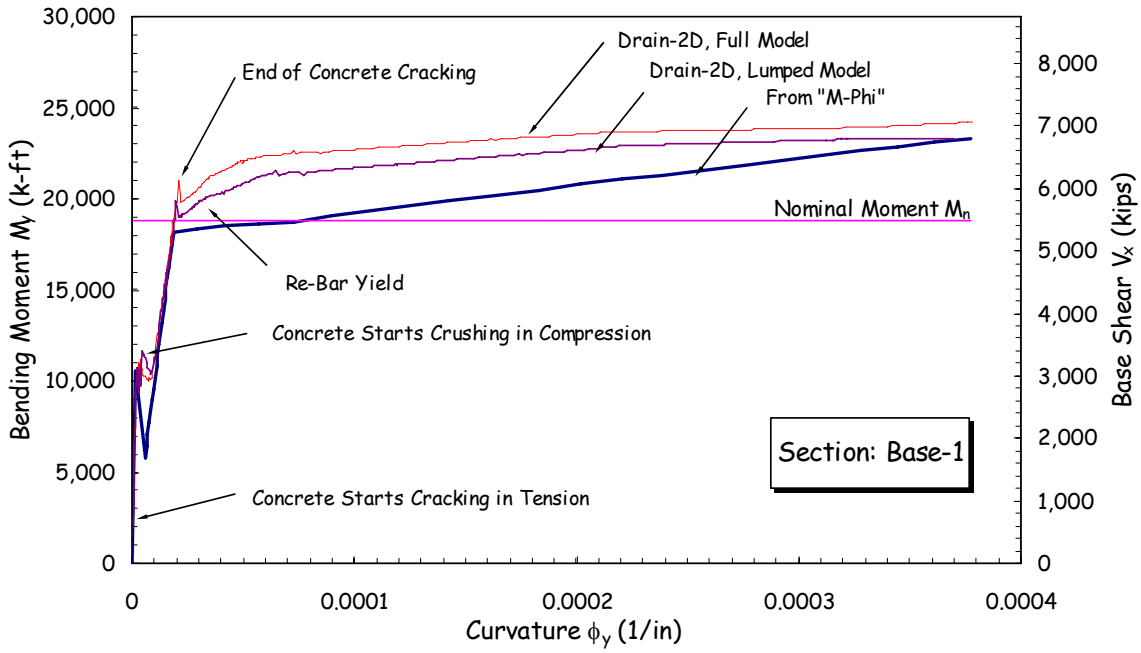

Figure E-12. Moment capacities and moment-curvature relationship of base slab from various procedures

c. Pushover Curve. In pushover analysis, the global response of the structure is commonly represented by a plot of the base shear versus lateral displacement. For the example lock, the plot of base shear versus a control node at the top of the lock wall is shown in Figure E-13 for both the Full and Lumped Models. Also shown in this figure and listed in Table E-4 are the base shear levels at which the soil begins yielding and 10%, 50%, 80%, or 100% of the piles experience yielding. Generally, the results of the Lumped and Full Models are in good agreement, except that the Lumped Model appears slightly stiffer than the Full Model (FigureE-13). This is probably due to bilinear approximation of the pile-head stiffness in the Lumped Model, which causes instant yielding as opposed to a gradual yielding with softening effect in the Full Model. The pile yielding for the Lumped Model is more sudden due to lumping nature of the pile-head stiffness. The first yielding in pile springs occurs at a lateral displacement of 3.5 cm (1.2 in.) and spreads to all pile springs at a lateral displacement of 5.31 cm (2.09 in.). While, in the case of Full Model, the first pile yielding starts at a lateral displacement of 5.34 cm (2.10 in.) and spreads to all piles at a much higher displacement of 15.81 cm (6.22 in.).

d. Percentage of Pile Yielding. Another interesting result is a graph of the base shear against the percentage of yielded piles, as shown in Figure E-14. This graph reveals that as soon as a few pile-head springs yield in the Lumped Model, the yielding spreads almost instantly to all other pile-head springs with no increase in the base shear. In the case of Full Model the pile yielding quickly spreads from a few percent to 75 percent of piles with very little increase in the base shear. However, the spread of yielding from 75 percent to 100 percent of the piles requires a significant additional base shear. For this example the pile-founded lock is considered safe and the level of damage acceptable if:

(1) The global displacement is not more than twice the first pile-yielding displacement

(2) The element or section curvature is not more than twice the section yield curvature

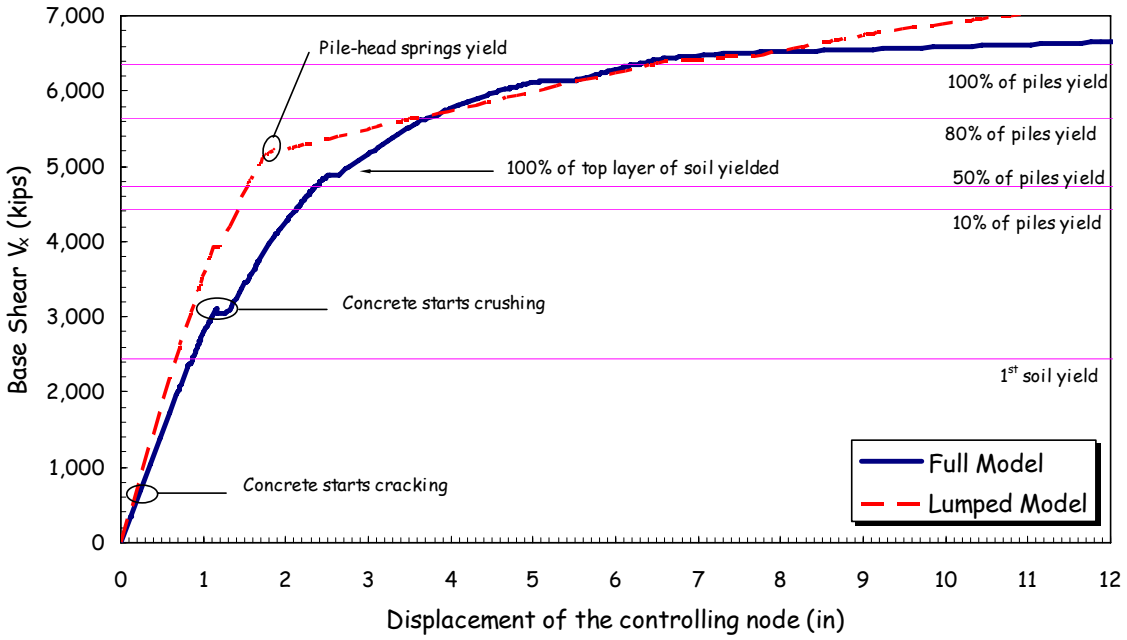

Figure E-13. Pushover curve indicating inelastic response (or level of damage) for Full and Lumped Models of example lock-pile system

Table E-4. Identification and estimate of damage for Full- and Lumped-Model representation of example lock-pile system

DAMAGE DESCRIPTION	FULL MODEL		LUMPED MODEL	
	Base Shear kN (kips)	Controlling Node Displacement cm (in)	Base Shear kN (kips)	Controlling Node Displacement cm (in)
1st Soil Yield	10,885 (2,447)	2.21 (0.87)		
1st Pile-Head Spring Yield			17,525 (3,940)	3.05 (1.20)
1st HP Pile Yield	19,564 (4,398)	5.34 (2.10)		
10% of Piles Yield	19,724 (4,434)	5.41 (2.13)		
30% of Piles Yield	20,349 (4,574)	5.67 (2.23)		
50% of Piles Yield	21,021 (4,725)	5.98 (2.36)		
100% of top soil layer yield	21,718 (4,882)	6.67 (2.63)		
10% of Pile-Head Springs Yield			22,438 (5,044)	4.29 (1.69)
65% of Pile-Head Springs Yield			22,817 (5,129)	4.40 (1.73)
100% of Pile-Head Springs Yield			23,346 (5,248)	5.31 (2.09)
80% of Piles Yield	25,054 (5,632)	9.45 (3.72)		
100% of Piles Yield	28,254 (6,351)	15.81 (6.22)		

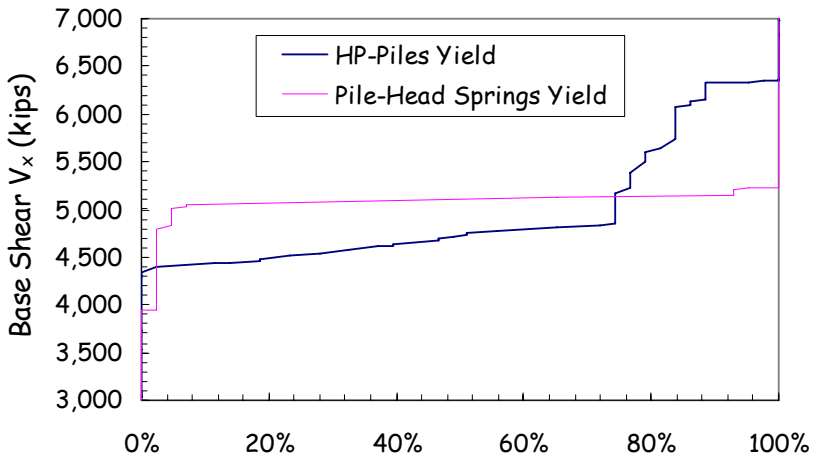

Figure E-14. Percent of Full Model piles and Lumped Model pile-head springs yielded vs. base shear

E-11. Conclusions and Recommendations

In general, lumped model representation of the pile foundation provides reasonable results, if pile-head stiffness properties are estimated accurately based on the single pile analysis discussed in this example and the coupling stiffness terms are considered in the analysis. If computation time is of no concern, the full model may be used for more accuracy. The full model also provides section forces and moments along the entire length of the piles, from which locations of maximum pile forces can be determined. The results show that the yielding spreads instantly from a few piles to more than 75 percent of the piles. Consequently, a sound acceptance criterion is to limit yielding to less than 10 percent of the piles.